Crystal structure and stability of the modulated composite Sb-II

Pressure-induced structural changes of antimony are a topic of both experimental and theoretical interest for more than 60 years. At low-pressures, Sb is isotypic to the ambient pressure phases of arsenic as well as bismuth. At a pressure of 8.5(5) GPa, antimony undergoes a reversible transformation into the high-pressure modification Sb-II. Further increase of pressure induces a transition into a cubic body centered arrangement (BCC) of antimony atoms at about 28 GPa [1–3]. The crystal structure of the high-pressure phase Sb-II is a long-standing matter of controversy. A tetragonal solution has been refined using powder diffraction data and resulted in a model with one type of Sb-atoms building up a three-dimensional framework and a second kind occupying every second tetragonal antiprismatic void in the resulting channels [1]. The close resemblance of this atomic arrangement to $CuAl_2$ type compounds (see Selected Research Reports) motivated the investigation presented here.

In accordance with earlier investigations, our measurements reveal pure patterns of the phase Sb-II at pressures above 13(1) GPa. Attempts to gain a conventional 3D-indexing solution of the diffraction pattern using automatic procedures fail. By application of the four-index method for composite structures a solution is obtained (see insert of Fig. 1) which comprises two tetragonal lattices with $a_c = 805.53(4)$ pm and two c-axes $c_h = 389.91(2)$ pm and $c_g = 297.33(4)$ pm. The common lattice parameter of both sub-structures is labeled a_c, the c-axis of the 'host' sub-lattice is termed c_h, and c_g corresponds to the c-axis of the 'guest' lattice. Systematic absences are compatible with two body centered sub-lattices. For the host, additional pseudo-extinction conditions of reflections $(0kl0)$: $k = 2n$ and $l = 2n$ are possible. However, overlap with reflections of the general type $(hklm)$ does not allow a definite determination of the systematic absences and three superspace groups remain compatible with the observations [5]. Beside the main reflections $(hkl0)$ and $(hk0m)$, the diffraction pattern contains weak first order satellite reflections $(hklm)$ fulfilling the extinction condition $h + k + l + m = 2n + 1$ with $m = \pm 1$, revealing a pronounced role of modulations in the crystal structure. The most prominent extra reflection in the pattern at $2\Theta \approx 8.15^o$ (see Fig. 1) is attributed to remaining low-pressure phase.

The sub-structures of host atoms Sb_h and guest atoms Sb_g were determined from Patterson functions calculated with the intensities of the $(hkl0)$ and $hk0m$ reflections, respectively. Atomic positions are compatible with three different superspace groups. In two of these groups under consideration, first order modulation waves of the Sb_g positions are not allowed. Thus, a complete refinement using full profiles including main reflections plus positions of the satellite reflections is performed in the remaining superspace group $L^{I422}_{-111}{:}L^{I422}_{-111}$ [6]. In order to calculate the intensities of the satellite reflections, the modulation functions for the Sb_h and Sb_g positions are created using a generator of the symmetry-allowed Fourier series. The structure refinement is performed in two steps. First, the average structure is refined. In a second step, the intensities of the satellite reflections are taken into account in order to optimize the parameters of the modulation functions. The refinement (Fig. 1) converges at $R_{\rm Br} = 0.088$ and $R_{\rm Pr} = 0.121$. The refined coordinate $x_h^{\rm av} = 0.15776(3)$ of the Sb_h atoms corresponds well to the value of 0.1536(3) obtained for the host species in the structurally closely related modification Bi-III at 6.8 GPa [4].

The most intriguing feature of the Sb-II crystal structure are condensed square antiprismatic columns of Sb_h atoms forming a three-dimensional framework. Figure 2 visualizes the crystal structure of Sb-II in two different projections. The selected representation emphasizes that the structural pattern of host and guest atoms is commensurate along the a-axes while the arrangement of atoms within the channels and the resulting misfit causes incommensuration along the c-axes.

The same characteristic atomic arrangement as that of the host atoms in Sb-II is observed in intermetallic phases of the $CuAl_2$ type. In Sb-II, the Sb_h sub-lattice corresponds to the configuration of aluminum atoms

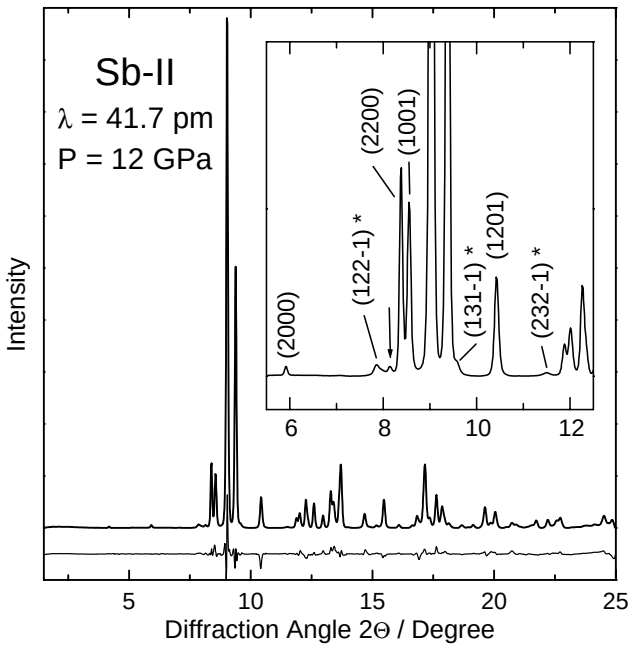

FIG. 1: Integrated x-ray diffraction profiles of Sb-II measured at $P = 12$ GPa and the difference between observed and calculated intensities. The inset shows the region of the pattern exhibiting the most intense reflections $(hklm)$ attributed to the modulation of atomic positions in both sub-structures (marked by asterisks). A single intense reflection which is tagged by an arrow is attributed to be the strongest line of a residual amount of low-pressure-phase Sb-I.

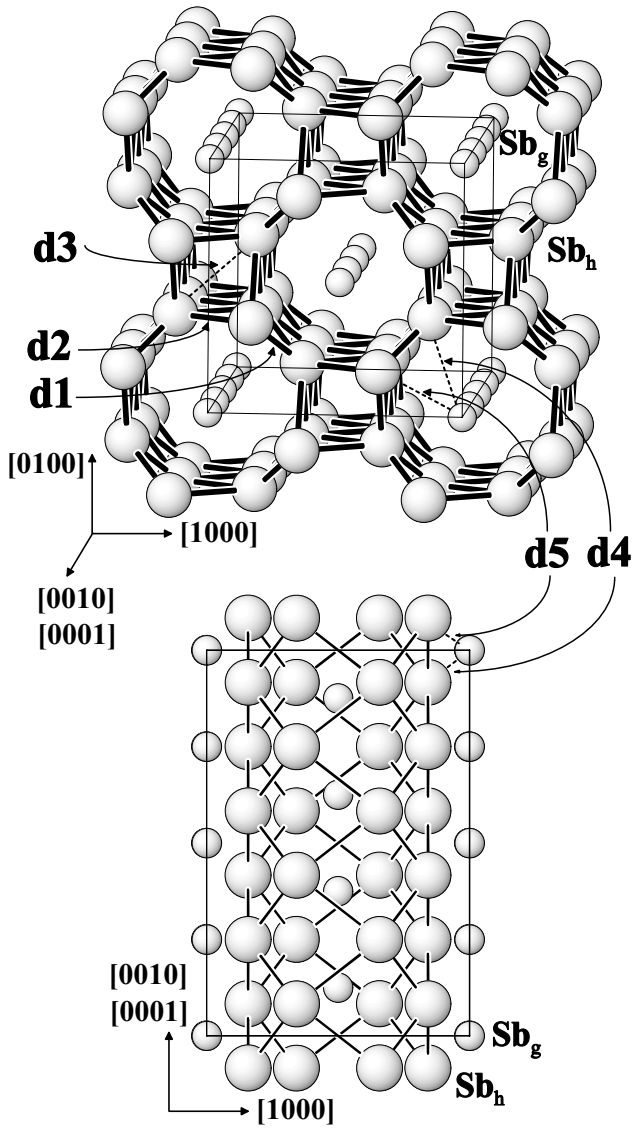

FIG. 2: Crystal structure of Sb-II shown in projections down the c-axes (top) and along the b-axis (bottom). Two tetragonal body centered sub-lattices realize a superstructure with common a-axes but different periodicity in direction of the c-axes.

in the crystal structure of $CuAl_2$ with a surprising similarity of the positional parameter of Al ($x = 0.1581$) to $x_h^{\rm av}$ of Sb_h. The resulting tubular assemblies of this sub-structure are occupied by a body-centered arrangement of guest atoms Sb_g. However, the copper atoms in $CuAl_2$ occupy all tetragonal antiprismatic voids whereas the Sb_g sublattice contains only slightly more than half the number of atoms corresponding to $(Sb_g)_{1-x}(Sb_h)_2$ with $x \approx 0.33$.

The finding of isotypic partial structures of $CuAl_2$ and antimony at high-pressures confirms the importance of intermetallic crystal structure types for high-density modifications of elements. The analoguous atomic organisation of an intermetallic compound and the structural pattern of Sb-II indicates a pressure-induced dissimilarity of chemically identical, but structurally different atoms.

The modulation of the Sb_h atoms facilitates a continuous adjustment of interatomic distances as a function of the common fourth coordinate $x4 = c_h/c_g \times z_h^{\rm av} = c_g/c_h \times z_g^{\rm av}$. For the interactions among host and guest atoms, $d4$ and $d5$, the modulated displacement of antimony atoms induces an additional reduction in the regime of short interatomic contacts and an elongation at long distances. The distances $d3$ located within tetrahedral chains connecting the antiprisms are significantly longer than strongly bonding contacts and, thus, are not supposed to represent robust covalent interactions of atoms Sb_h. The interatomic spacing between neighboring guests within the same channel falls into the range of the majority of minimal interatomic antimony distances. This finding is taken as an indication of a pronounced influence of intra-channel interactions between antimony atoms on the lattice parameter c_g.

Every atom Sb_g has two neighbors in the channel with a distance of approximately 297 pm. Two extreme situations mark the coordination range of Sb_g: The lower limit of CN 6 is realized when the guest species is coordinated by four host atoms in the center of a square ($x4 = \pm\, 0.5$), the upper limit of CN 10 corresponds to a location of Sb_g in the center of the square antiprisms of Sb_h ($x4 = 0$) like it is found for the ideal Cu position in

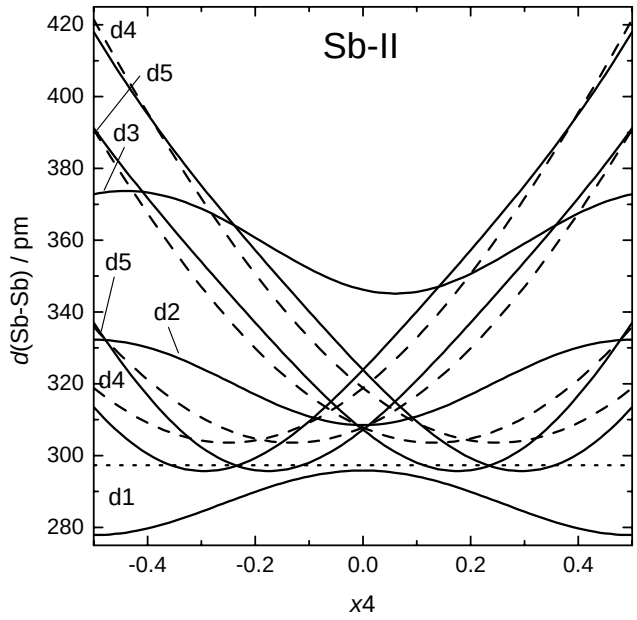

FIG. 3: Interatomic distances of Sb-II at $P = 12$ GPa as a function of the fourth coordinate $x4$. Dashed lines represent distances calculated for a non-modulated structure, full lines correspond to those of the modulated atomic arrangement, and the dotted line reproduces the distance between channel atoms.

the $CuAl_2$ structure. Thus, the coordination polyhedra of Sb_g are formed by two channel atoms Sb_g plus 4 (+4) atoms Sb_h (distances $d4$ and $d5$ in Fig. 2 and Fig. 3). The host atoms Sb_h have CN 8 and are coordinated by six framework atoms (distances $d1$ and $d2$) plus two channel atoms Sb_g ($d4$ and $d5$). Within the stability region of the modification Sb-II, the axial ratio c_h/c_g changes by less than 0.4 % and does not achieve the next higher rational value 4/3 which would result in a commensurate structure with the smallest possible common lattice parameter c of guest and host lattice. However, we will use this commensurate *approximant* of the modulated composite which reproduces the basic features of the atomic organisation adequately as a model structure for the total energy calculations.

The crystal structures being considered as models for the total-energy calculations are restricted to the experimentally evidenced modifications of antimony or varieties thereof: (i) the rhombohedral structure (A7), (ii), simple cubic (sc; cubic primitive), (iii) body-centered cubic (BCC), (iv) the tetragonal arrangement (TP) with P4/n symmetry proposed earlier [1], and (v) an *approximant* of the incommensurate composite (TA) suggested in this work, tetragonal with P4 symmetry.

The results of the total energy calculations are summarized in Fig. 4. The results concerning energy and volume are normalized by the number of atoms in the unit cell in order to facilitate a straightforward comparison of the investigated structure types. The zero energy is chosen as the energy minimum of the idealized composite (TA) with P4 symmetry approximating the incommensurately modulated structure proposal. The results for the two independent calculation schemes agree with respect to the calculated equlibrium volumes within less than 1% for all investigated structure types. The corresponding total energy differences (referred to the TA structure) agree up to several hundredth mHartree except for the A7 structure where we find a slight offset of both curves, probably due to numerical differences caused by the different handling of crystal symmetries in both methods. The excellent agreement of two independent methods is taken as a strong evidence for the reliability of the calculational results.

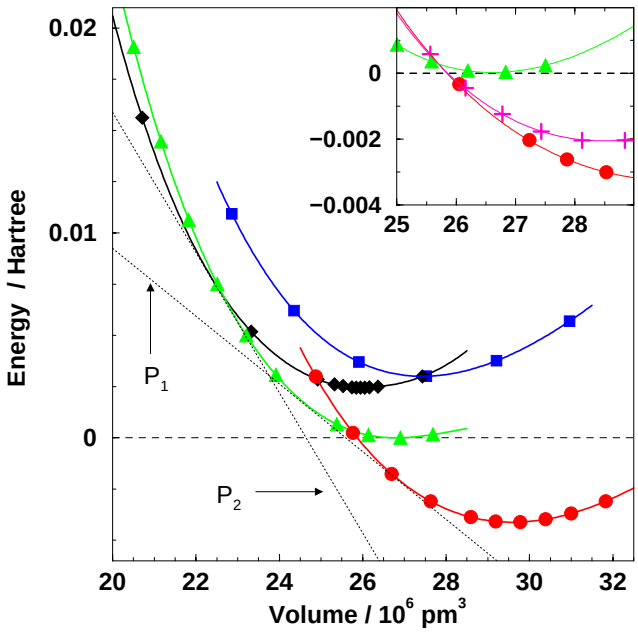

FIG. 4: Energy versus volume per atom for the different structures under investigation. The calculated energies are marked by symbols. A7: circles; tetragonal approximant (TA): triangles; tetragonal primitive (TP): squares; BCC: diamonds. Insert: Crosses represent simple cubic. Solid lines are cubic splines fitted to the calculated data. The dashed lines are tangents to the energy-volume curves according to the Helmholz construction illustrating the transition pressures.

In order to reduce the required computing time, the c/a-ratio of the tetragonal structures are fixed to the experimental values. For the A7 type, we optimized the c/a-ratio for the equlibrium volume and kept the value fixed in the subsequent calculations since its influence on the total energies is negligible. In contrast, the total energy is significantly affected by changes of the positional parameter. Thus, the internal coordinate, z, of the A7 structure is optimized at each calculated point. As can be seen from Fig. 4 the sequence of phase transitions predicted by the calculations is in perfect agreement with the experimental findings. At pressures up to about 8.7 GPa the A7 structure is stable. As shown in the inset of Fig. 4, the SC structure lies higher in energy at low pressures. The energy differences between A7 and SC decrease with increasing pressure and becomes exceedingly small near the Sb-I - Sb-II phase transition region. In accordance with experimental results, the total energy calculations evidence that a different crystal structure emerges before the SC arrangement becomes more stable than A7. For volumes less than about 22 $\times 10^6$ pm^3 (corresponding to about 75% of the theoretical equilibrium volume of 29.7 10^6 pm^3) the BCC structure has the lowest energy, in complete accordance with the results of previous experiments. In the region between these phases, the approximant (labeled TA) is the most stable atomic arrangement. The TP structure suggested earlier [1] is found to be quite high in energy (almost three mHartree per atom higher in energy than the approximant). Consequently, the total-energy calculations definitely rule out this structure as a possible Sb-II modification.

In order to provide a quantitative measure between experimental and theoretical findings, we show experimental data in comparison to the theoretical pressure-volume curve (Fig. 5). The theoretical values are obtained from Birch-Murnaghan type equations of state. Since measured and calculated volumes match almost perfectly (ambient pressure: 30.1 $\times$ 10^6 pm^3 versus 29.7 $\times$ 10^6 pm^3, respectively), both data sets are plotted by using absolute volumes rather than scaled values. The agreement between theory and experiment is excellent for the Sb-I phase and the Sb-III modification.

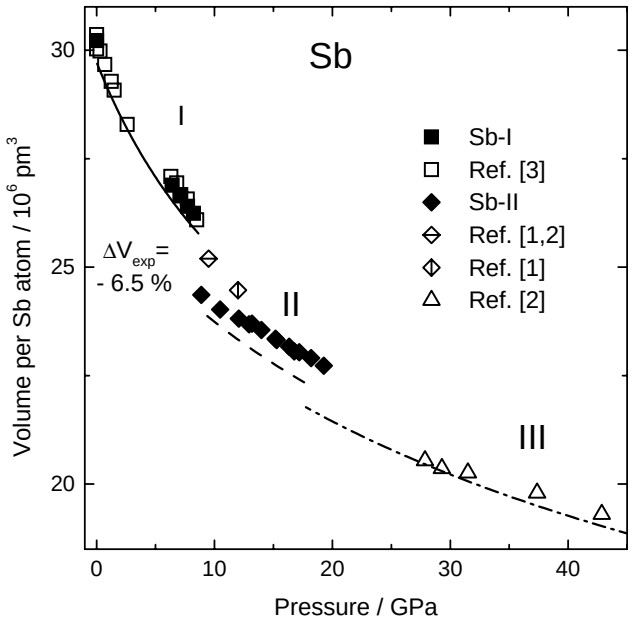

FIG. 5: Volume per antimony atom at pressures up to 42 GPa. Solid symbols represent data from the present investigation; open icons indicate values taken from literature. Curved lines represent Birch-Murnaghan-type equations fitted to the results of the quantum mechanical calculations.

Note that for Sb-II, a commensurate approximant is used instead of the actual incommensurately modulated composite. Nevertheless, the transition pressure of 8.7 GPa, and the volume decrease of 5.9% (with respect to theoretical volume) are in sound accord with the experimental data. The transition pressure for the Sb-II to BCC transition is predicted to be smaller: 17.7 GPa calculated versus 28 GPa measured.[2]
The proposed structural model for the high-pressure phase Sb-II allows for the first time an integrated description of both main and satellite reflections in an x-ray powder diffraction pattern of an incommensurately modulated atomic assembly of a main group element. The structure changes in antimony at high-pressures were modelled by quantum mechanical calculations (FPLMTO and FPLO). We obtain excellent agreement between the calculated and experimentally determined sequence of structural phase transitions and pressure-volume relations. Moreover, on the basis of the calculated total energies we can discard an earlier proposed crystal structure in favour of an approximant developed on the basis of the four-dimensional model. The present investigation of Sb-II evidences that the interaction between the two incommensurate atomic arrangements in one crystal structure induces modulated atomic displacements of atoms in both sub-lattices and leads to a surprisingly complex structural organization of atoms in a chemical element. The structural similarity to the host-guest structures of the high-pressure modifications of bismuth, barium and strontium indicates the importance of incommensuration and modulation for element structures. We expect that high accuracy experimental techniques for structure solution and refinement, even from x-ray powder diffraction data, in combination with sophisticated theoretical methods will shed new light on the phase diagrams of chemical elements.

Ulrich Schwarz, Lev Akselrud, Helge Rosner, Alim Ormeci, Yuri Grin und Michael Hanfland (ESRF, Grenoble)

[1] H. Iwasaki and T. Kikegawa, High Pressure Res. **6**, 121 (1990).
[2] K. Aoki, S. Fujiwara, and M. Kusabe, Solid State Commun. **45**, 161 (1983).
[3] D. Schiferl, D. T. Cromer, and J. C. Waber, Acta Crystallogr. B**37**, 807 (1981).
[4] M. I. McMahon, O. Degtyareva, and R. J. Nelmes, Phys. Rev. Lett. **85**, 4896 (2000).
[5] L^{I422}_{-111}:L^{I422}_{-111}, L^{I4cm}_{111}:L^{I4mm}_{111}, or $L^{I4/mcm}_{1-111}$:$L^{I4/mmm}_{1-111}$
[6] Equivalent positions: (0,0,0,0; 1/2,1/2,1/2,1/2) + $x1, x2, x3, x4$; $x1, -x2, -x3, -x4$; $-x2, -x1, -x3, -x4$; $x2, x1, -x3, -x4$; $-x1, -x2, x3, x4$; $-x1, x2, -x3, -x4$; $x2, -x1, x3, x4$; $-x2, x1, x3, x4$.